Available online at www.sciencedirect.com
ScienceDirect
Journal of the European Ceramic Society 29 (2009) 2783–2789
www.elsevier.com/locate/jeurceramsoc

Fe_2O_3-doped forsterite ceramics as a joining partner for ZrO_2 in a laser brazing process

F. Heilmann [a,b,*], G. Rixecker [a], F.D. Börner [b], W. Lippmann [b], A. Hurtado [b]

[a] *Robert Bosch GmbH, Corporate Sector Applied Research and Advance Engineering, Stuttgart, Germany*
[b] *Technische Universität Dresden, Institute of Power Engineering, Dresden, Germany*

Received 8 October 2008; received in revised form 22 March 2009; accepted 31 March 2009
Available online 19 May 2009

Abstract

Gastight, high-temperature stable sealing between yttria-doped zirconia (ZrO_2) and an electrically insulating ceramic joining partner is necessary for a wide range of applications in oxygen sensing and energy conversion. To accomplish this, laser brazing with glass solders is an attractive alternative to existing joining processes. Due to a near-perfect match of its thermal expansion with the one of ZrO_2 up to high temperatures (∼800 °C) and good thermal and electrical insulation properties, forsterite (Mg_2SiO_4) is chosen as a candidate joining partner. As the absorptivity of pure forsterite at the used diode laser wavelengths of 808 and 940 nm is quite low, increasing the energy absorption by doping forsterite with Fe_2O_3 appears to be a promising refinement of this technique. The optical properties of the resulting olivine ceramics are evaluated. The results show that Fe_2O_3-doped forsterite is both suitable as a joining partner for ZrO_2 and for tuning its absorptivity.

Keywords: ZrO_2; Joining; Thermal expansion; Optical properties; Sensors

1. Introduction

Ceramics require special manufacturing processes which are different from metals or polymers. In many cases, it is suitable to choose simple, modular geometries and to join them after sintering, especially if undercuts are necessary.[1] Apart from their hardness, a main advantage of ceramic materials is their stability to high temperatures and corrosive media which makes them ideal for protecting parts more susceptible to these influences. To avoid weak points, the joint has to fulfil these requirements as well.

For the purpose of creating a high-temperature stable, gas tight joint between ceramic parts, two main possibilities exist, i.e. brazing and welding.[2] Ceramic welding would imply joining temperatures of 1700–2300 °C as the ceramic material itself has to be molten. This would affect the grain structure adversely and would lead to excessively high thermal stresses due to the high coefficient of thermal expansion (CTE).

In contrast, the joining temperatures required for brazing can be rather close above the application temperature, as an intermediate material is used to permanently contact both materials. Some glasses are especially suitable to join ZrO_2 parts for high-temperature applications. These are mostly alkaline earth silicate systems.[3,4]

Sugar et al.[5] propose two liquid-film joining method for alumina ceramics with metallic interlayers which either disappear via interdiffusion or promote the formation of ceramic/metal interlayers. Goretta et al.[6] give a review on plastic deformation joining for various oxide ceramics. This method is scrutinized by Yang et al.[7] for the purpose of zirconia-based electrochemical sensors as well.

As compared to a batch process using a furnace, laser brazing in the described work is desirable because it provides an increased flexibility in the design of the manufacturing process. As oxide and some silicate ceramics are highly transparent at common diode laser wavelengths of 808 and 940 nm, volume absorption is possible with these materials, heating up the whole ceramic part rather than the surface only. Apart from alleviating the thermal shock issues, this also enables hidden brazing areas

* Corresponding author at: BERU AG, Advance R&D, 71636 Ludwigsburg, Germany. Tel.: +49 170 1013016.
E-mail address: felizitas.heilmann@beru.com (F. Heilmann).

0955-2219/$ – see front matter © 2009 Elsevier Ltd. All rights reserved.
doi:10.1016/j.jeurceramsoc.2009.03.028

(covered, e.g. by one of the joining partners) to be reached. With suitable solder materials this is possible with microwave heating as well, as described by Loehman[8] yet buried metallic heating elements would be easily damaged.

The suitability of a laser joining process for non-oxide ceramics, especially silicon carbide, was proven by Lippmann et al.[9] Due to their high strength potential and low CTE non-oxide ceramics such as SiC and Si_3N_4 are well suited to endure thermal shock due to either temperature transients or stationary temperature gradients. High thermal conductivity helps flatten temperature gradients applied, e.g. by a localised laser heating process. The primary objective of the present work is to apply the same type of process to oxide ceramics (which are more susceptible to thermal shock), in order to obtain gas tight joints in ceramic gas sensors or energy converters such as solid oxide fuel cells based on the oxygen ion conductor ZrO_2.[10]

A zirconia-based sensor is able to withstand temperatures in excess of 800 °C and is highly stable in corrosive atmospheres. Its fixture has to fulfil the same requirements of chemical resistance in aggressive media. Yet this material has to be electrically insulating also at elevated temperatures to electrically separate the zirconia ceramic from conductive materials, especially metals in the periphery.

A commonly used oxide ceramic material which would fulfil the electrical requirements is alumina. However, due to a high mismatch in CTE in excess of 3 ppm/K, alumina is not the first choice for this purpose. A magnesium silicate ceramic, forsterite (Mg_2SiO_4), is likely to be better suitable. Its CTE is close to that of zirconia (see Fig. 1), especially at temperatures up to the ones used in the joining process,[11,12] and the electrical resistivity at elevated temperatures is sufficiently high, as shown in Fig. 2, which was determined in pre-experiments with an in-house setup at Robert Bosch GmbH. Thus the combination of zirconia and forsterite may be ideal for fixing the sensor in its housing. The very low absorptivity of forsterite in the spectral range of diode lasers was shown in advance tests. Doping of glass with FeO as a means to increase the absorption coefficient was already mentioned by Scholze.[13] As Mg_2SiO_4 and

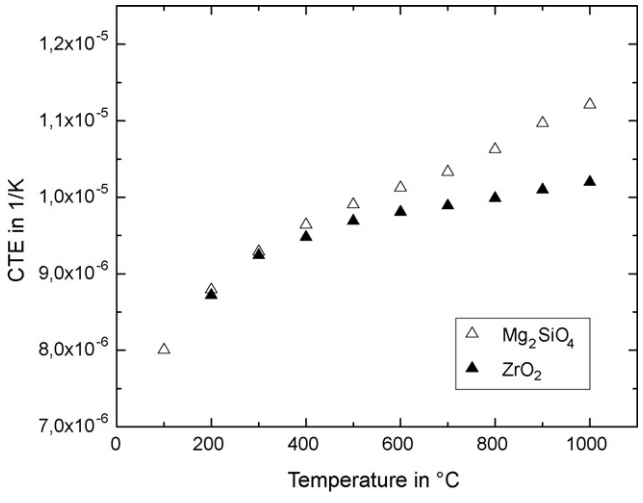

Fig. 1. Comparison of the CTE of ZrO_2 and Mg_2SiO_4.

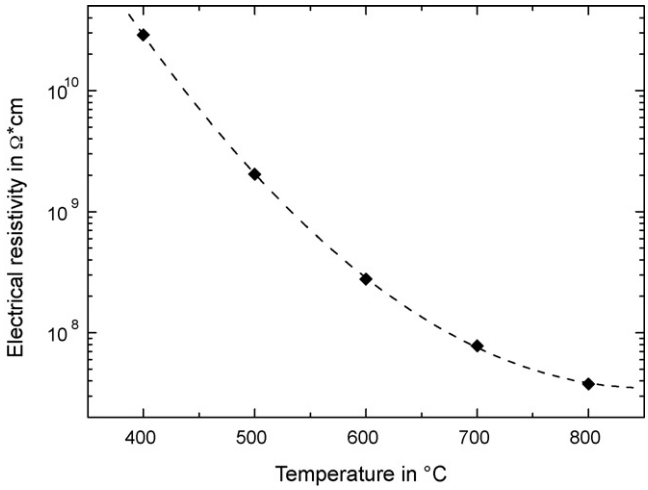

Fig. 2. Temperature-dependent electrical resistivity of Mg_2SiO_4.

fayalite (Fe_2SiO_4) occur naturally together in olivine minerals,[14] Fe oxide can be assumed to be a suitable dopant for forsterite. Manufacturing routes for forsterite ceramics are described by Alecu and Stead.[15] The aim of the following experiments is to prove the tunability of the absorptivity of forsterite ceramics in the relevant wavelength spectrum.

2. Experimental

2.1. Preparation of the forsterite/fayalite ceramics and soldering glass

In order to make forsterite ceramics with tailored optical properties it is necessary to prepare the samples from highly pure synthetic raw materials. In the present study synthesis was accomplished by a reaction sintering process. As the reaction sintering is facilitated by a high surface-to-volume ratio, fine-grained powders of MgO, Fe_2O_3 and SiO_2 (Nos. 105866, 103924 and 113126, Merck KGaA, Darmstadt, Germany) were chosen. MgO and SiO_2 were mixed in a molar ratio of 2.0:1.0, as this corresponds to the Mg_2SiO_4 stoichiometry. Fe_2O_3 was added in amounts of 0.0, 0.1, 0.5 and 1.0 wt.% based on the Mg-content of Mg_2SiO_4. The nomenclature "wt.% Fe" is used in this sense. The powders were mixed with ethyl alcohol to obtain a viscous slurry which was then homogenised for 1 h at 600 rpm in a laboratory dissolver (Dispermat AE04-C1, VMA-Getzmann GmbH, Reichshof, Germany). The powder mixtures were dried for 10 h at 20 °C followed by a final drying step at 40 °C and 20 kPa.

Uniaxial pressing of the powder was done at 60 MPa with a ramp of 5 MPa/s and 10 s dwell time. A shaping die with an external diameter of 17.0 mm and an internal diameter of 5.5 mm was used to press disks with a central hole.

The samples were then sintered at 1600 °C for 5 h with a ramp of 100 K/h. The sintering parameters were obtained by preliminary tests. In the same way disks without a hole were prepared for characterisation purposes. XRD measurements were performed to confirm that practically all of the raw material components are

converted to Mg_2SiO_4 or Fe_2SiO_4 during the reaction sintering process.

The yttria-stabilised ZrO_2 (8 wt.% yttria) that is used as a joining partner for the forsterite discs was provided in the form of rods with a diameter of 4 mm and a length of 60 mm (FZY, Friatec GmbH, Mannheim, Germany). Its density is 5.85 g/cm^3.

The soldering glass was prepared from raw powders of Al_2O_3, B_2O_3, BaO, L_2O_3, SiO_2 and SrO which were mixed with ethyl alcohol and homogenised in a speedmixer (DAC 400 FVZ, FlackTek Inc., Landrum, SC, USA) at 800 rpm for 1 min and 2000 rpm for 4 min. The slurry was dried for 10 h at 20 °C, followed by 5 h at 80 °C. Premelting of the powder mixture was done at 1250 °C with a 5 K/min ramp and 30 min dwell time. An elevator furnace (Agni GmbH, Aachen, Germany) was used which enables rapid unloading of the hot platinum crucible with the molten glass. The glass ingots were quenched in water at about 20 °C which led to their fragmentation. The dried glass chips were then milled in a planetary ball mill (PM 100, Retsch GmbH, Haan, Germany). Two milling steps of 20 min each were performed, using 3 and 14 agate grinding balls of 20 and 10 mm diameter, respectively. As a result, a mean particle size of $d_{50} = 4.5$ μm is obtained. The glass frits were pressed into rings and pellets which were sintered to guarantee mechanical stability in the laser brazing process. Due to the fast heating during laser brazing, it is not possible to use organic binders. The rings were sintered onto the ZrO_2 rods at 700 °C for 30 min to better adapt to the tolerances of the ceramic parts.

2.2. Laser brazing process

A 3.1 kW diode laser with two different infrared wavelengths, 808 and 940 nm (Rofin Sinar, Hamburg, Germany) is used in continuous wave (cw) mode. The absorptivity of common oxide ceramics, including alumina, stabilised zirconia and forsterite, is rather low in this spectral range.[16] This property can be exploited for a volume absorption process, as enough energy for joining can be transported inside the material over a distance of millimetres to centimetres. In this way thermally induced stress can be kept at a significantly lower level compared to surface heating alone. Moreover, hidden brazing zones are reached owing to the semi-transparency of the samples. The present laser brazing process is performed with sample rotation at 200 rpm with energies between 50 and 500 W, the ZrO_2 joining partner being clamped between two synchronously rotating fixtures. This setup leads to an improved homogeneity of the energy input and is useful for parts with joining zones having axial symmetry. The temperature of the parts is obtained during the laser process via a thermo camera (VarioCAM, Infratec GmbH, Dresden, Germany), which was calibrated on the high-temperature emissivity of the ceramics before.

2.3. Characterisation methods

2.3.1. Sintering behaviour

Changes in porosity P and density ρ of the sintered samples can be used to monitor the influence of Fe_2O_3 additions on the sintering behaviour. ρ was obtained from the mass m and the geometrically obtained volume V of the samples after sintering:

$$\rho = \frac{m}{V}.$$

ρ can be compared with the theoretical density ρ_{th} of forsterite and fayalite to return the porosity, as follows:

$$P = \left(1 - \frac{\rho}{\rho_{th}}\right) \times 100$$

2.3.2. Coefficient of thermal expansion

The coefficients of thermal expansion (CTE) of the ceramic materials were determined via dilatometric measurements (Netzsch DIL 402C, Netzsch GmbH, Selb, Germany) on ceramic rods cut from the sintered disks. The heating rate in these measurements was 5 K/min. The standard deviation of the temperature measurement is ±1 K.

2.3.3. Optical properties

With UV/VIS/NIR-spectrometry (Lambda UV/VIS/NIR spectrometer, PerkinElmer Inc., Waltham, MA, USA) reflexion and transmission can be measured in a wavelength range between 200 and 2500 nm. The intensity I_0 of the incident beam, the reflected or backscattered fraction I_R and the transmitted or forward-scattered fraction I_X are related as (with x as the sample thickness and k as the absorptivity):

$$I_x = (I_0 - I_R) \cdot e^{(-x \cdot k)}.$$

By this measurement, the absorptivity changes due to Fe_2O_3 addition can be detected.

3. Results and discussion

3.1. Material characterisation

3.1.1. Thermal and mechanical properties

The CTE of the sintered forsterite ceramics is $1.33 \pm 0.016 \times 10^{-5}$/K between 20 and 1000 °C without any dependence on Fe_2O_3 addition. The glass' CTE was measured as $1.21 \pm 0.02 \times 10^{-5}$/K. Glasses and ceramics have a higher compressive strength than tensile strength.[17] The tensile strengths of glasses are commonly lower than those of ceramics. In a joint geometry as depicted in Fig. 3, the ceramic disk with a higher CTE than both the glass and the ceramic rod induces compressive stress in the joining zone under during cooling. Thus the tensile stress necessary to break the weakest part of the assembly is higher than without such a pre-compression.

The obtained porosity of the forsterite ceramics is 11.6 ± 0.9% for the material with 0 wt.% Fe and 10.8 ± 1.2% for 1.0 wt.% Fe. Considering the standard deviation, the porosity is not changed by the Fe_2O_3 addition.

3.1.2. Optical properties

Measurements of the optical properties were performed to assess the influence of doping the ceramic material with Fe_2O_3.

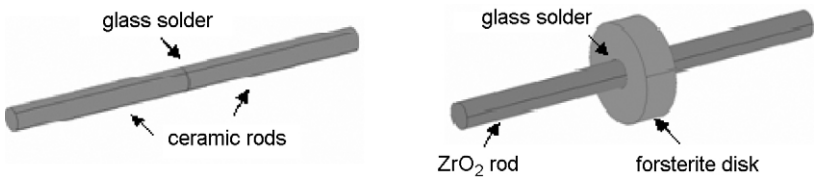

Fig. 3. Schematic drawing of the geometries used for the laser brazing process.

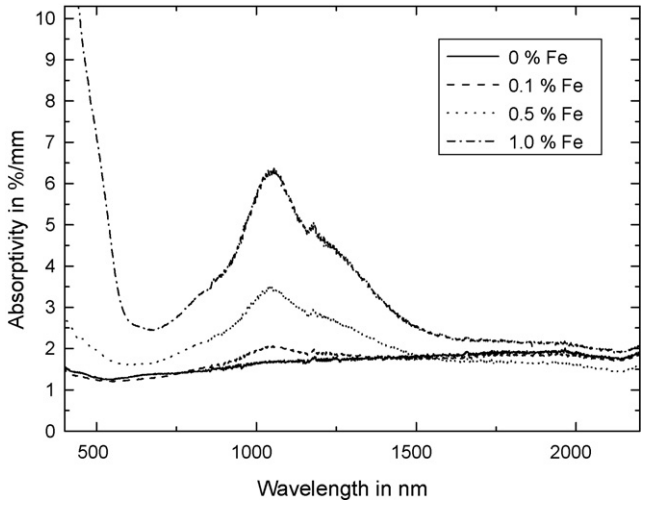

Fig. 4. Absorptivity spectra of Mg_2SiO_4 with 0.0–1.0 wt.% Fe.

The spectra are depicted in Fig. 4, showing the appearance of an absorptivity peak between 700 and 1500 nm wavelength which increases with higher Fe_2O_3 addition. Standard deviation of the measurement device resolution is ≤0.005 nm in the UV/VIS-range and ≤0.02 nm in the NIR. Due to stray light, a wavelength dependent standard deviation of ≤0.00007–0.0005% is possible. For the laser wavelengths of 808 and 940 nm the values can be seen in Fig. 5. With $R^2 = 0.999$ the graphs can be fitted exponentially according to $y = A\exp(x/t) + y_0$ with Table 1.

This enables tuning the absorptivity of forsterite between 1.44%/mm for 0 wt.% Fe and 3.2%/mm for 1.0 wt.% Fe at the laser wavelength of 808 nm, and 1.49–4.4%/mm at the wavelength of 940 nm. The type of fitting is proposed due to the exponential influence of damping factors k on the transmitted beam intensity I as described in 2.3.

Table 1
Fitting parameters to Fig. 5 for laser wavelengths of 808 nm and 940 nm.

	808 nm	940 nm
y_0	0.46	−0.16
A	0.96	1.74
t	0.95	1.03

3.2. Joining experiments

3.2.1. Changes in joining time and thermal gradients by increasing the absorptivity

Joining time, necessary laser power and thermal gradients are strongly influenced by changing the absorptivity of the forsterite ceramics. Average laser power for joining forsterite disks to ZrO_2 rods was 400 W for forsterite without Fe_2O_3-addition and could be reduced to 285 W for the material with 0.1 wt.% Fe and to 95 W when using the forsterite ceramic with 1.0 wt.% Fe. Although laser power was reduced, the necessary time for joining still could be shortened from 343 ± 80 to 152 ± 36 and 145 ± 13 s. To highlight the effect of both parameters, Fig. 6 shows the quantity (joining time × laser power) for the three forsterite ceramics. The greatest decline in time and power happens between 0.0 and 0.1 wt.% Fe.

Radial thermal gradients in the forsterite disk were measured from thermo camera images. The thermal gradient was obtained

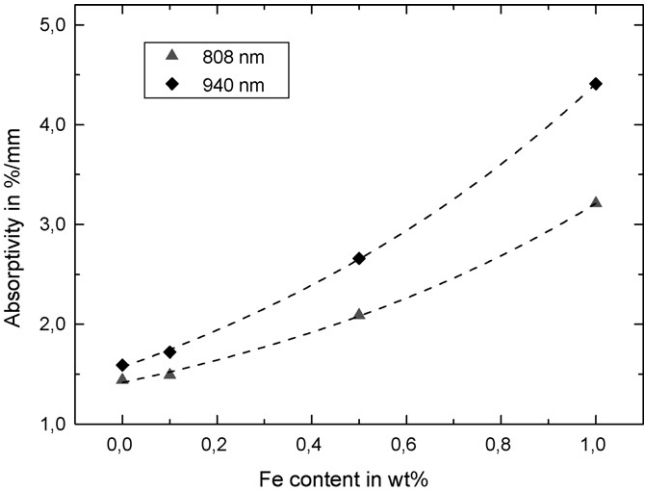

Fig. 5. Absorptivity at the laser wavelengths.

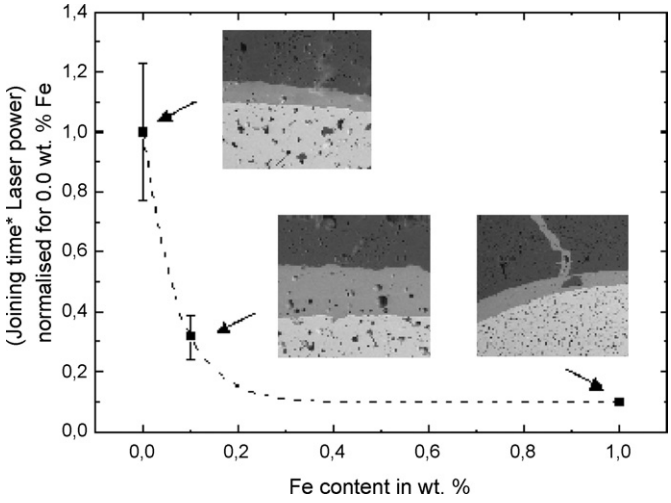

Fig. 6. Effect of doping the basic forsterite with Fe_2O_3.

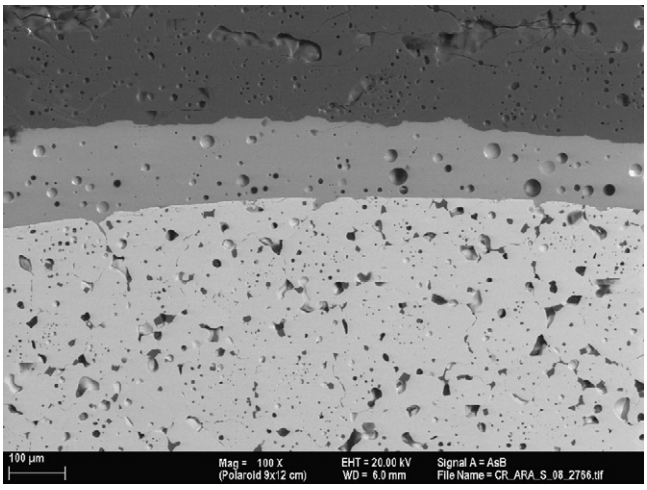

Fig. 7. Zirconia joined to forsterite doped with 0.1% Fe.

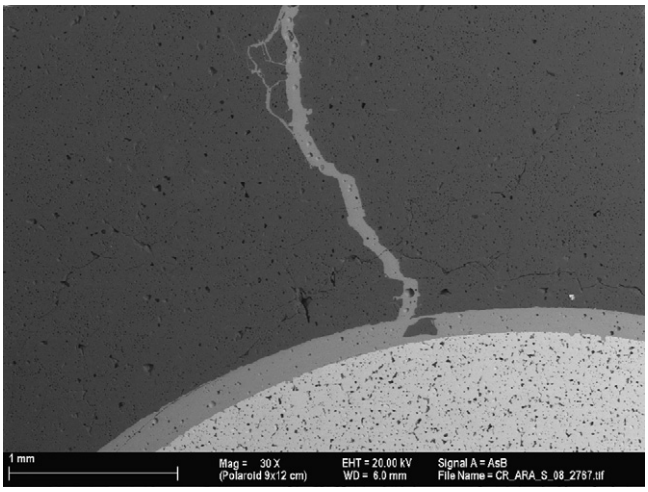

Fig. 8. Zirconia joined to forsterite doped with 1.0% Fe.

along a line over a length of 4.7 mm from the outer surface of the forsterite disk to the inner surface. The gradient was taken when the inner boundary of the disk had reached the joining temperature of 1250 °C. 22 K/mm were measured for the forsterite ceramic without Fe_2O_3-addition. The forsterite ceramic with a Fe-content of 0.1 and 1.0 wt.% have a thermal gradient of 52, respectively 67 K/mm. This means temperatures at the outer surface of 1355, 1470 and 1540 °C. The effect of the thermal gradients is discussed below, corresponding to the scanning electron microscopy (SEM) images.

3.2.2. SEM and WDX analysis of the joined area

The thumbnail images in Fig. 6 show the resulting joining zone of zirconia (light grey) to forsterite (dark grey). The images of 0.0 and 0.1 wt.% Fe show the same good quality of the joined area. The depicted details for 0.1 and 1.0 wt.% Fe are fully displayed in Figs. 7 and 8. The forsterite ceramic doped with 0.1 wt.% Fe results in a crack free joint. Radial cracks appear in the forsterite ceramic doped with 1.0 wt.% Fe due to the occurrence of too large thermal gradients. The outer surface has a much higher temperature than the inner surface, leading to tensile stresses due to the thermal expansion. Another possible explanation might be residual stresses during cooling, leading to parallel compressive stresses in the zirconia, leading to tensile stresses in the forsterite bonding region. For detailed investigations on residual stresses in joint zones, see Gutierrez-Mora et al.[18] As can be seen in Fig. 8, the molten glass fills the crack. This means, in this case the crack is rather due to thermal gradients during laser joining.

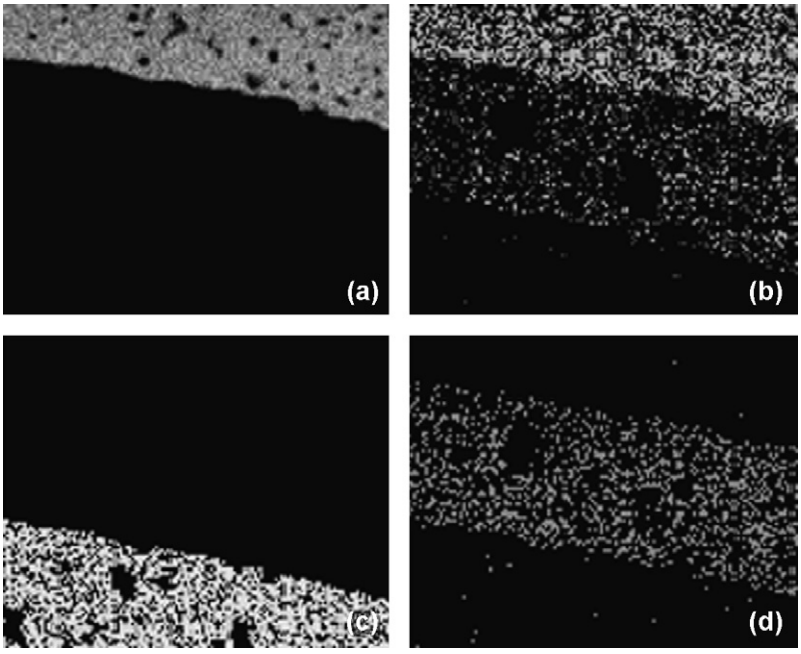

Fig. 9. WDX element distribution: (a) Mg, (b) Si, (c) Zr and (d) B.

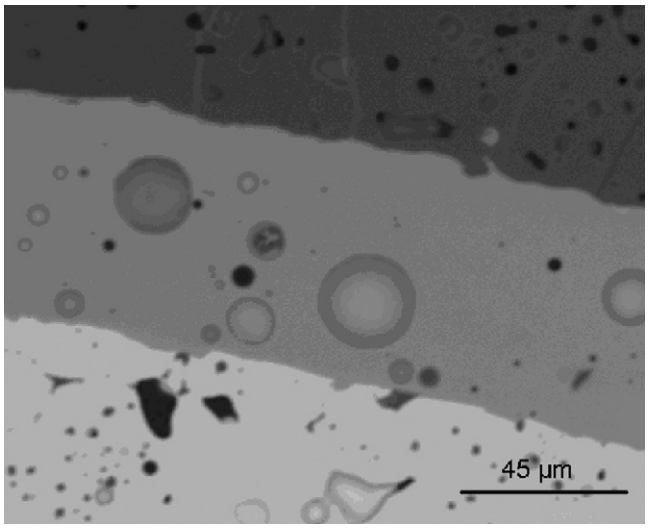

Fig. 10. SEM micrograph used for WDX analysis in Fig. 9.

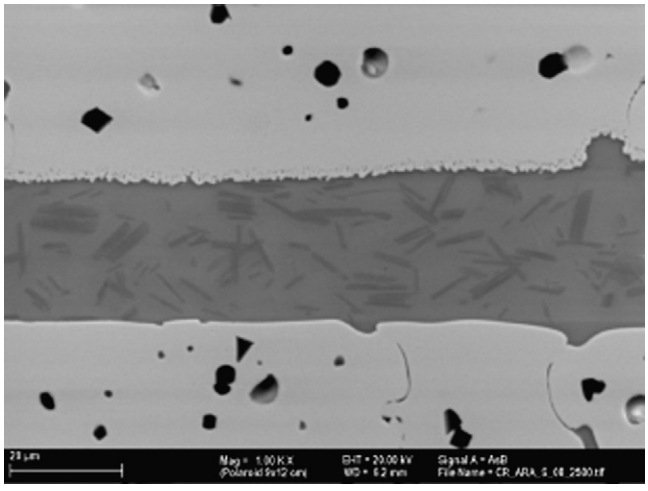

Fig. 11. ZrO_2–ZrO_2 joint made via a laser joining.

Wavelength dispersive analysis (WDX) shows that the joining time is sufficiently short to prevent ions from diffusing from the glass into one of the ceramic joining partners or vice versa (Fig. 9, corresponding SEM image given in Fig. 10). Especially boron as a rather mobile species is kept from diffusing (Fig. 9d). That is why the other contained elements can be supposed not to be diffusing either, especially Fe whose amount was below the detection limit. Due to these limits, minimal diffusion may have occurred for all contained elements. To compare the influence of short-term laser heating and longer annealing times on the structure of the glass–ceramic interface, rod samples were coated with glass slurry on one side and annealed in the furnace for 30 min at 1100 °C. Fig. 11 shows a laser-brazed ZrO_2–ZrO_2 joint using a glass-coated and pre-annealed upper rod and an unglazed one in the lower side of the micrograph. A 2 µm thick reaction zone on the furnace-annealed ceramic–glass interface is evident, whereas no reaction zone can be detected on the side that was only laser heated. Thick reaction zones may be suitable, as materials gradients lead to property gradients and thus, e.g. help reducing stresses. In this case, it is preferable to have no reaction zones, as these seem to introduce three-dimensional defects in the material contact area as can be seen in Fig. 11.

4. Conclusion

It has been shown that forsterite-based ceramics are highly suitable as a joining partner for zirconia, especially in a laser brazing process based on volume heating, for a couple of reasons:

- Both oxide and silicate ceramics have good wetting to special borosilicate glasses.
- The short heating period in a laser process is suitable to prevent diffusion and undesired interaction between the joining partners.
- By adding Fe_2O_3 to the raw powder mixture, the absorptivity of the forsterite ceramic can be tuned.
- Fe_2O_3-dopant concentration of 0.1 wt.% Fe is a good compromise for reducing joining time, laser power and thermal gradients.

References

1. Eagar, T. W., Baeslack, W. A. and Kapoor, R., Joining of advanced materials. In *Encyclopedia of Advanced Materials*, *1207*, ed. D. Bloor, M. Flemings, R. Brook and S. Mahajan, 1994.
2. Messler, R. W., Joining of engineered ceramics. *Advanced Materials and Processes*, 2004, **162**(11), 43–45.
3. Lahl, N., Bahadur, D., Singh, K., Singheiser, L. and Hilpert, K., Chemical interactions between aluminosilicate base sealants and the components on the anode side of solid oxide fuel cells. *Journal of the Electrochemical Society*, 2002, **149**(5), 607–614.
4. Geasee, P., *Entwicklung von kristallisierenden Glasloten für planare Hochtemperatur-Brennstoffzellen*. Aachen, RWTH Aachen, Fakultät für Bergbau, Hüttenwesen und Geowissenschaften, 2003.
5. Sugar, J. D., McKeown, J. T., Akashi, T., Hong, S. M., Nakashima, K. and Glaeser, A. M., Transient-liquid-phase and liquid-film-assisted joining of ceramics. *Journal of the European Ceramic Society*, 2006, **26**(4–5), 363–372.
6. Goretta, K. C., Singh, D., Chen, N., Gutierrez-Mora, F., de la Cinta Lorenzo-Martin, M., Dominguez-Rodriguez, A. *et al.*, Microstructure and properties of ceramics and composites joined by plastic deformation. *Materials Science and Engineering A*, 2008, **498**(1–2), 12–18.
7. Yang, J.-C., Spirig, J. V., Karweik, D., Routbort, J. L., Singh, D. and Dutta, P. K., Compact electrochemical bifunctional NO_x/O_2 sensor with metal/metal oxide internal reference electrode for high temperature applications. *Sensors and Actuators B*, 2008, **131**(2), 448–454.
8. Loehman, R. E., Recent progress in ceramic joining. *Key Engineering Materials*, 1999, **161–163**, 657–662.
9. Lippmann, W., Knorr, J., Wolf, R., Rasper, R., Exner, H., Reinecke, A. M. *et al.*, Laser joining of silicon carbide—a new technology for ultra-high temperature resistant joints. *Nuclear Engineering and Design*, 2004, **231**, 151–161.
10. Holtappels, P., Vogt, U. and Graule, T., Ceramic materials for advanced solid oxide fuel cells. *Advanced Engineering Materials*, 2005, **7**(5), 292–302.
11. Sembach GmbH, Lauf, Germany, personal note, 2006.
12. Friatec AG, Mannheim, Germany, personal note, 2006.
13. Scholze, H., *Glas: Natur, Struktur und Eigenschaften*. Springer Verlag, Berlin, 1977.
14. Okrusch, M. and Matthes, S., *Mineralogie*. Springer Verlag, Berlin, 2005, pp. 420–421.

15. Alecu, I. D. and Stead, R. J., Development of forsterite ceramic materials at rojan advanced ceramics. *Journal of the Australian Ceramic Society*, 1998, **34**(2), 50–53.
16. Touloukian, Y. S. and DeWitt, D. P., Thermal radiative properties: nonmetallics solids. In *Thermophysical Properties of Matter, the TPRC Data Series, a Comprehensive Compilation of Data*, *8*, ed. Y. S. Touloukian. IFI/Plenum, New York, 1972.
17. Askeland, D. R., *The Science and Engineering of Materials, PWS Series in Engineering*. PWS Publishing Company, Boston, MA, US, 1994.
18. Gutierrez-Mora, F., Goretta, K. C., Majumdar, S., Routbort, J. L., Grimdisch, M. and Dominguez-Rodriguez, A., Influence of internal stresses in superplastic joining of zirconia toughened alumina. *Acta Materialia*, 2002, **50**(13), 3475–3486.